ISTITUTO NAZIONALE DI FISICA NUCLEARE

Sezione di Milano

INFN/TC-83/7
7 Marzo 1983

G. Bellomo and L. Serafini: A STUDY OF THE MAGNETIC FORCES ACTING ON THE TRIM COILS, FOR THE MILAN SUPERCONDUCTING CYCLOTRON

Servizio Documentazione
dei Laboratori Nazionali di Frascati

Istituto Nazionale di Fisica Nucleare
Sezione di Milano

INFN/TC-83/7
7 Marzo 1983

G. Bellomo and L. Serafini: A STUDY OF THE MAGNETIC FORCES ACTING ON THE TRIM COILS, FOR THE MILAN SUPERCONDUCTING CYCLOTRON

1. - INTRODUCTION.

A three sectors superconducting cyclotron, with a K = 800 and a K_{FOC} = 200, is under construction at the University of Milan. The machine is designed as a booster for a 16 MV Tandem with ultimate energies between 100 MeV/n for fully stripped light ions down to 20 MeV/n for uranium and intensities in the range 10^{10}-10^{11} particles/sec. A detailed report on the project has been published elsewhere(1).

The machine will operate with average magnetic fields between 22 and 48 kGauss; the trimming of the field is obtained by the independent excitation of the two main coil sections (each one carrying up to 3500 A/cm^2) and by 20 trim coils wound around the hills (with a max excitation of 4000 ampereturns each).

The operating diagram of the machine in the (B_o, Z/A) plane, i. e. the center field value and the charge to mass ratio, is presented in Fig. 1. The bending and focusing limits, together with the constant energy per nucleon lines, are shown. Also listed is the trim coil power for the representative ions.

The aim of this paper is to evaluate the forces acting on the trim coils because of the cyclotron magnetic field.

Four trim coils, out of twenty, have been selected as representative of the entire set and the corresponding distribution of the forces has been computed.

The results obtained are presented in some detail and their implications for the design of the mechanical structure of the trim coils are discussed.

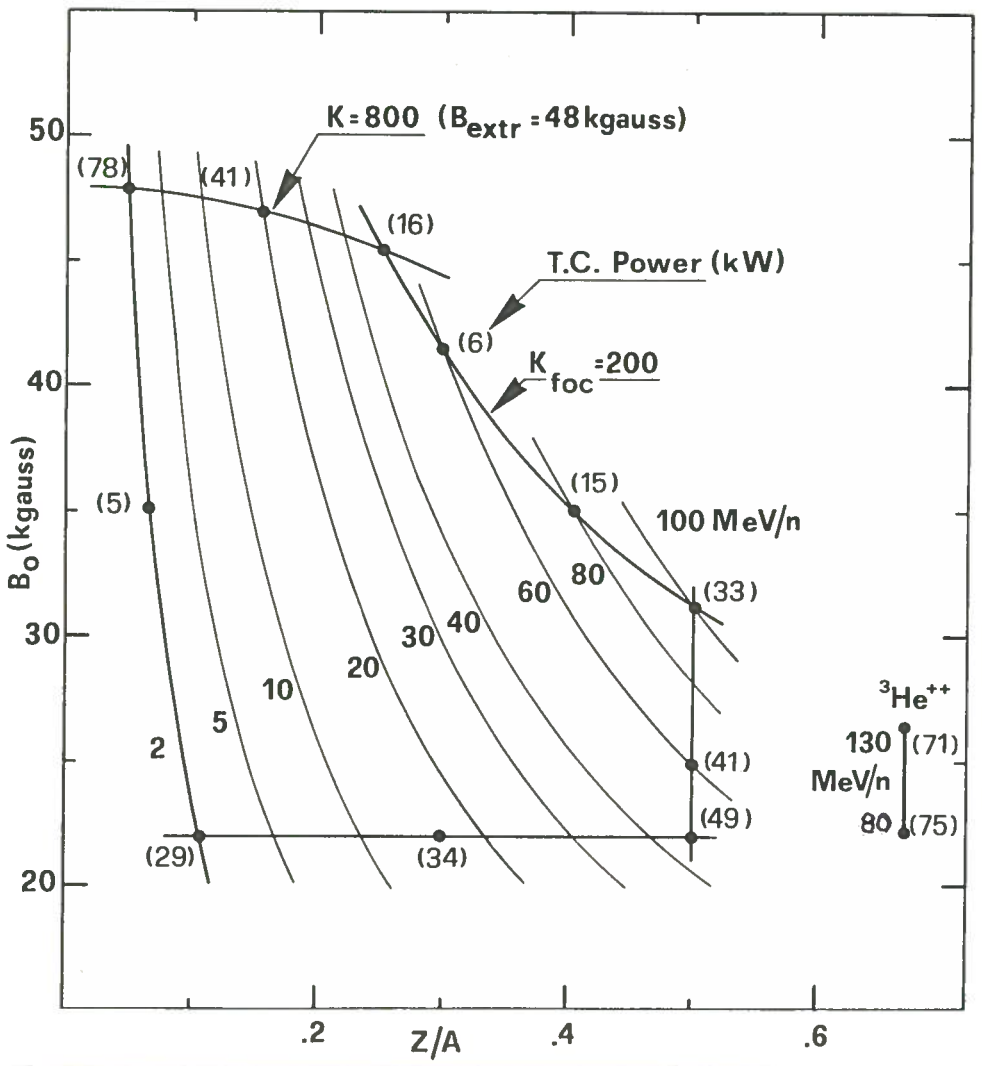

FIG. 1 - Operating diagram in the (B_o, Z/A) plane.

2. - THE TRIM COILS GEOMETRY.

A schematic top view of the cyclotron and of the hills and valleys profile is presented in Figs. 2 and 3 respectively.

The azimuthal width of the hill is 33^o at R = 9 cm and reaches 46^o at R = 40 cm being then constant up to R = 72 cm. There the hill width increases reaching 52^o at R = 86.7. From R = 86.7 to R = 90 cm the hill has no spiral angle in order to better control the onset of the resonance $\nu_r + 2\,\nu_z = 3$ (see Ref. (1)). Each hill profile is defined by three arcs of circles which have, two by two, a common point of tangency.

The twenty trim coils are wound on the upper part of the hill and are packed in five groups, of 4 coils each, separated by radial spacers which also support the hill as indicated in Fig. 4.

The hill is rounded at the edges with a 20 mm radius of curvature in order to facilitate the winding of the trim coils, which have there a 18 mm radius of curvature.

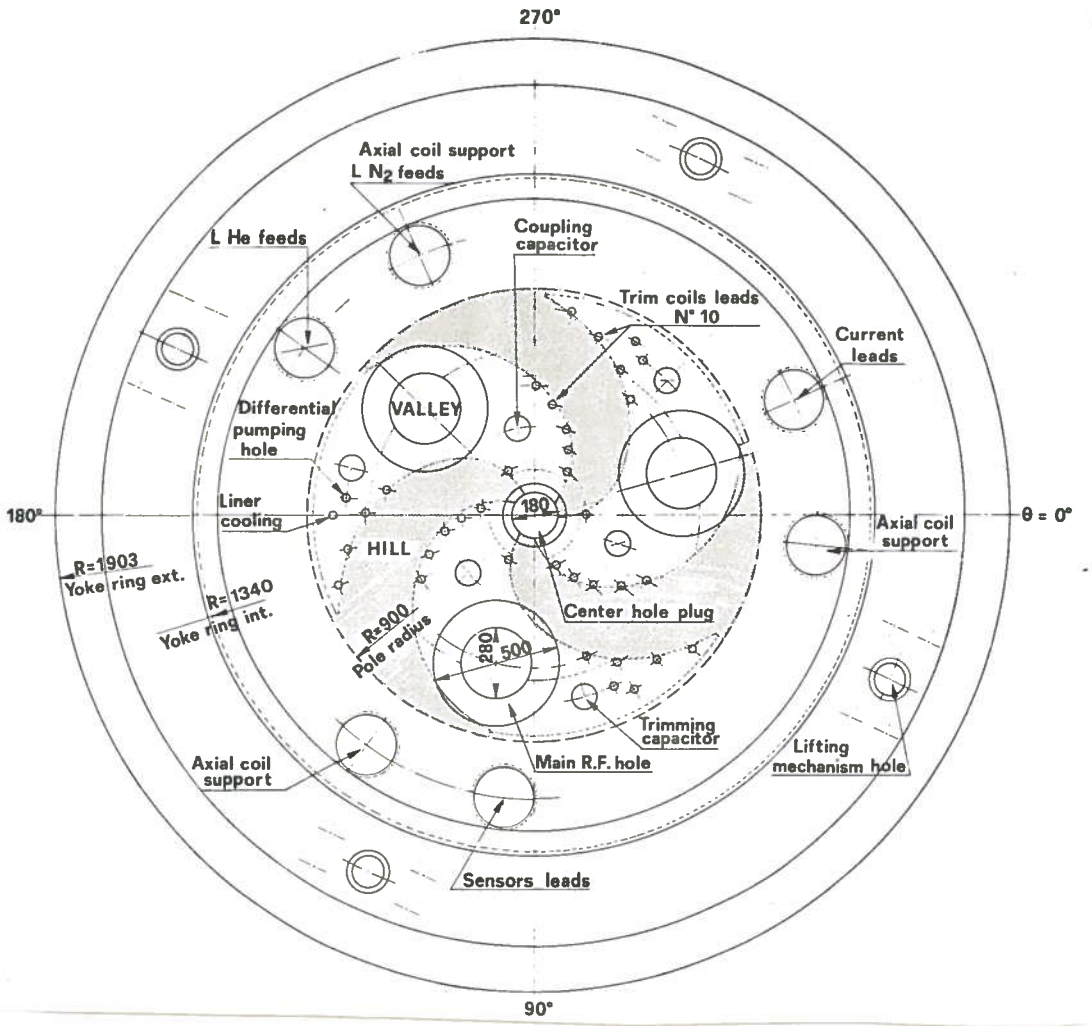

FIG. 2 - Sketch of the magnet from the top (All dimensions in cm).

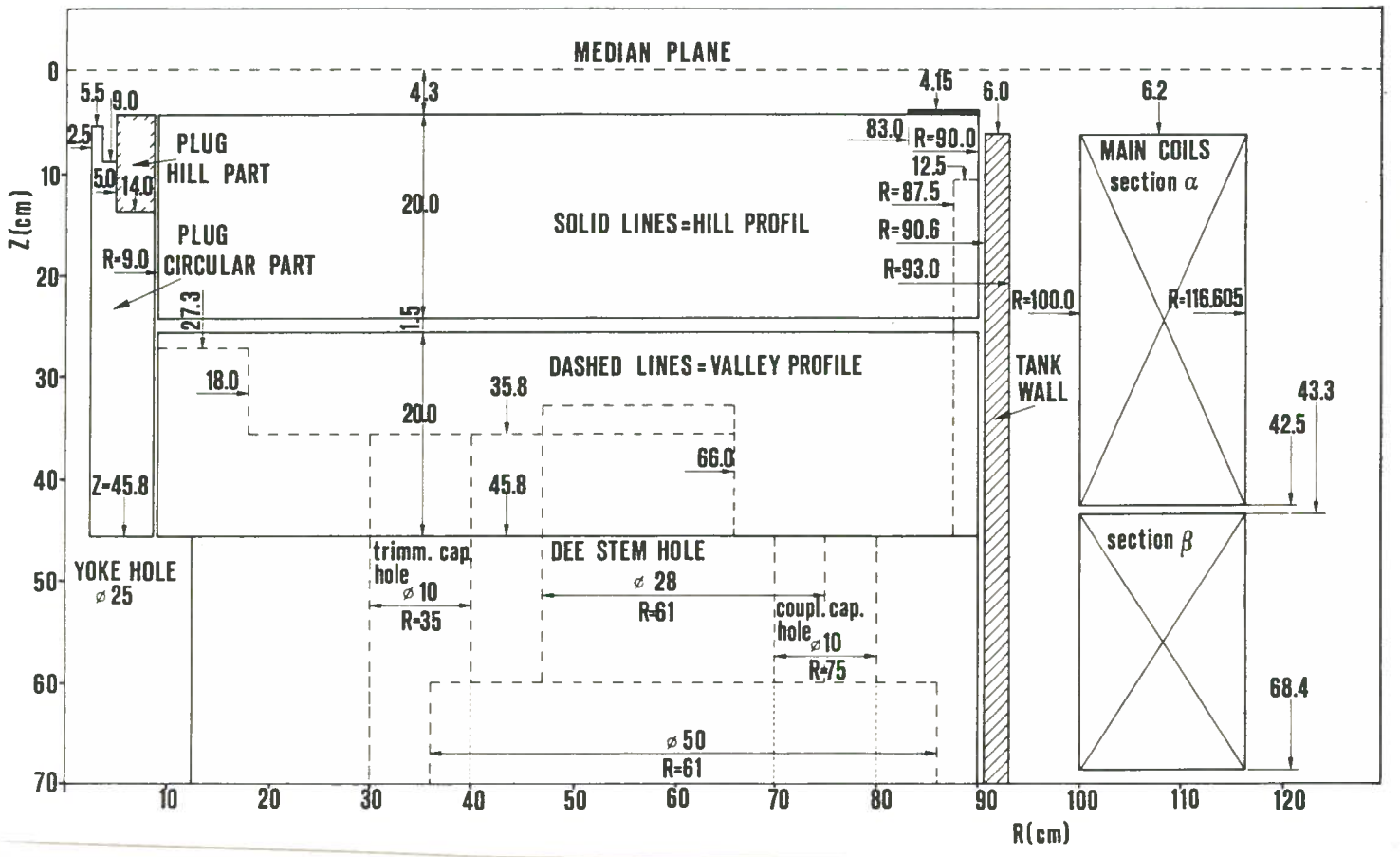

FIG. 3 - Hill and Valley radial profile (All dimensions in cm).

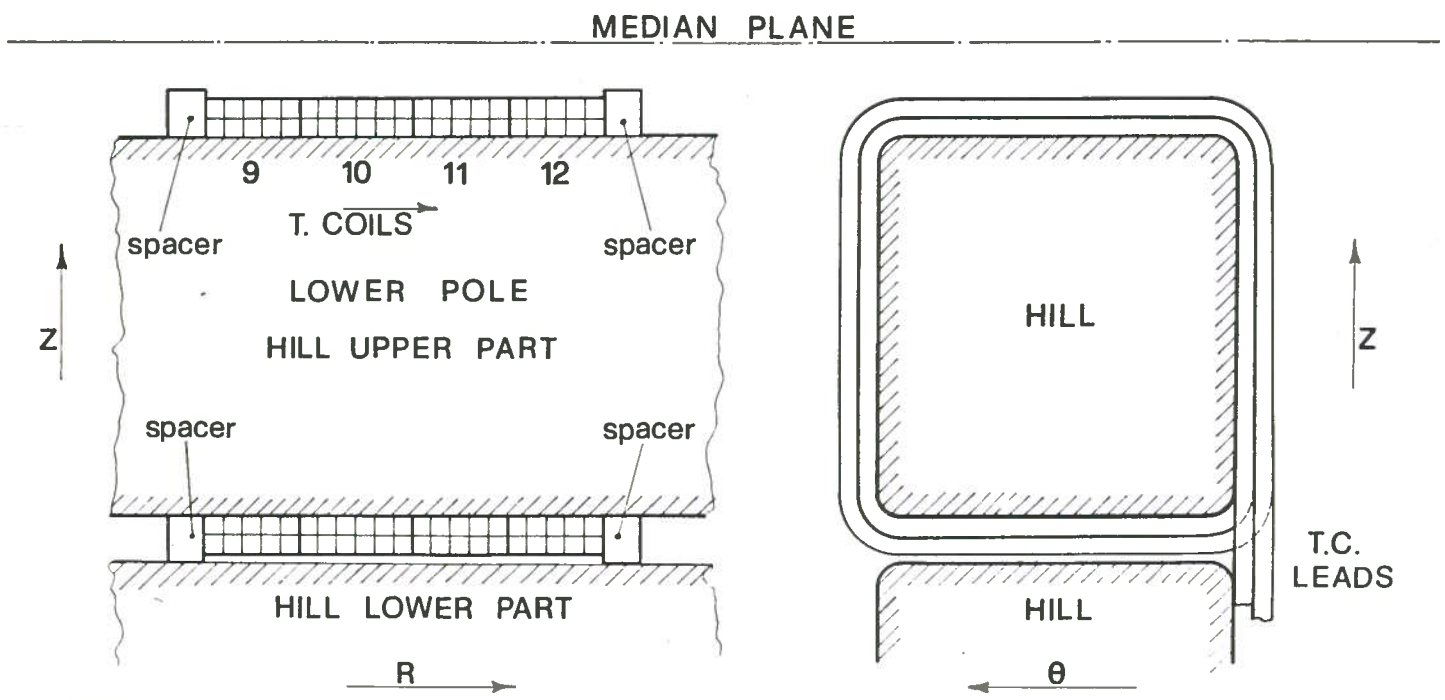

FIG. 4 - Schematic view of a group of four trim coils.

Each trim coil consists of two layers with a variable number of turns to fill up completely the region between the spacers. The last coil has only one layer to allow the inward movement of the electrostatic deflector. The entrance and exit leads lay on the same side of the hill; for each group of two trim coils four leads go through the same hole on the valley floor so that ten holes per hill are provided for this purpose (see Fig. 2).

The trim coils are wound with 1/4" square hollow (ϕ = 3/16") copper conductor which can carry up to 500 A. The group of 4 coils closest to the center uses however a 3/16" square hollow (ϕ = 1/8") conductor in order to limit the azimuthal extent of the trim coils on the hill side. This will allow a gap to gap azimuthal width, between the dees as close as possible to the design value of 60^{o}.

Trim coils number (1, 2) or (3, 4) and (19, 20) will be used also as harmonic coils to control the first harmonic in the injection and the extraction regions. The maximum excitation needed for the trimming of the field has been calculated in 4000 At and about 1600 At are required for harmonic mode operation. The main characteristics of the trim coils are listed in Table I.

3. - MAGNETIC FIELD CALCULATION.

The evaluation of the forces acting on the trim coils requires first the calculation of the magnetic field in the volume occupied by the coils, according to the formula

$$\vec{F} = \int_V \vec{J} \times \vec{B} \, dv$$

where $\vec{F}$ is the total force acting on the volume V, $\vec{J}$ is the current density and $\vec{B}$ is the magnetic field.

TABLE I - Trim coils geometry.

T. C.	RAV (cm)	R_I (cm)	R_F (cm)	$\Delta\vartheta$ (deg)	Nt	I (A)	Notes
		9.00	9.80				Spacer 0
1	11.59	9.80	13.38	42.1	14	400	
2	15.17	13.38	16.95	44.3	14	400	Harmonic coils
3	18.74	16.95	20.53	45.6	14	400	Conductor 3/16"
4	22.32	20.53	24.11	46.5	14	400	
		24.11	25.41				Spacer 1
5	27.08	25.41	28.76	48.0	10	400	
6	30.77	28.76	32.77	48.3	12	330	
7	34.45	32.77	36.12	48.5	10	400	
8	37.80	36.12	39.47	48.5	10	400	
		39.47	40.77				Spacer 2
9	42.46	40.77	44.14	48.4	10	400	
10	46.16	44.14	48.19	48.2	12	330	
11	49.87	48.19	51.56	48.1	10	400	
12	53.24	51.56	54.93	48.1	10	400	
		54.93	56.23				Spacer 3
13	57.92	56.23	59.60	48.0	10	400	
14	61.62	59.60	63.65	47.9	12	330	
15	65.33	63.65	67.02	47.9	10	400	
16	68.70	67.02	70.39	48.0	10	400	
		70.39	71.69				Spacer 4
17	73.38	71.69	75.08	48.1	10	400	
18	76.77	75.08	78.47	48.5	10	400	
19	80.50	78.47	82.53	49.7	12	460	Harmonic coil
20	84.57	82.53	86.60	51.1	6	500	Harmonic coil, one layer
		86.60	87.90				Spacer 5

RAV — Average radius of the trim coil

R_I, R_F — Initial and final trim coil radii

$\Delta\vartheta$ — Average azimuthal width of the trim coil

Nt — Number of turns of the trim coil

I — Maximum excitation current (trimming and harmonic operation mode).

We replace the real coil cable with a linear wire located at the center of its cross section and carrying the nominal cable current I so that the formula given above is reduced to

$$\vec{F} = \Sigma \int_L \vec{I} \times \vec{B} \, dl$$

where L is the length of the coil and the sum extends over all the trim coil cables.

Since the current $\vec{I}$ is directed either along the ϑ or z direction (see Fig. 4) only two magnetic field components need to be evaluated for each side of the loop. In the space between the poles, the total field $\vec{B}$ is the sum of the following three terms:

$$\vec{B}(r, \vartheta, z) = \vec{B}_c(r, z) + \vec{B}_s(r, \vartheta, z) + \vec{B}_y(r, z)$$

where

$\vec{B}_c$ is the field produced by the main coils (air core field);

$\vec{B}_s$ is the field produced by the poles and the sectors;

$\vec{B}_y$ is the field produced by all other iron volumes and indicated here as yoke contribution.

All the three terms depend in principle from the main coils excitation. However the poles and the pole sectors are in practice quite close to saturation and therefore their contribution can be calculated using the uniform saturation approach[2]. The yoke field contribution can be calculated with the code POISSON by reducing the three dimensional iron structure to a bidimensional one through the use of reduced permeability values[3]. The validity of this approach has been tested for the MSU K500 cyclotron in the median plane and the agreement with the measured data is quite satisfactory[4]. We therefore assume that this procedure is valid also for the region outside the median plane.

Unfortunately the data supplied by the code POISSON outside the median plane and close to the iron surfaces are not very reliable. This is in part due to the grid size used in that region and mostly to the fact that the code POISSON uses the vector potential $\vec{A}$ and therefore the evaluation of $\vec{B}$ close to the iron surfaces becomes somewhat critical. We are then forced to use a zeroth-order approximation for the yoke field contribution, namely

$$\vec{B}_y(r, z) = \vec{B}_y(r, 0)$$

where $z = 0$ indicates the midplane.

The B_y field contribution at the midplane is presented in Fig. 5 for two different excitations of the two main coils sections (see Fig. 3 for the definition of the α and β section).

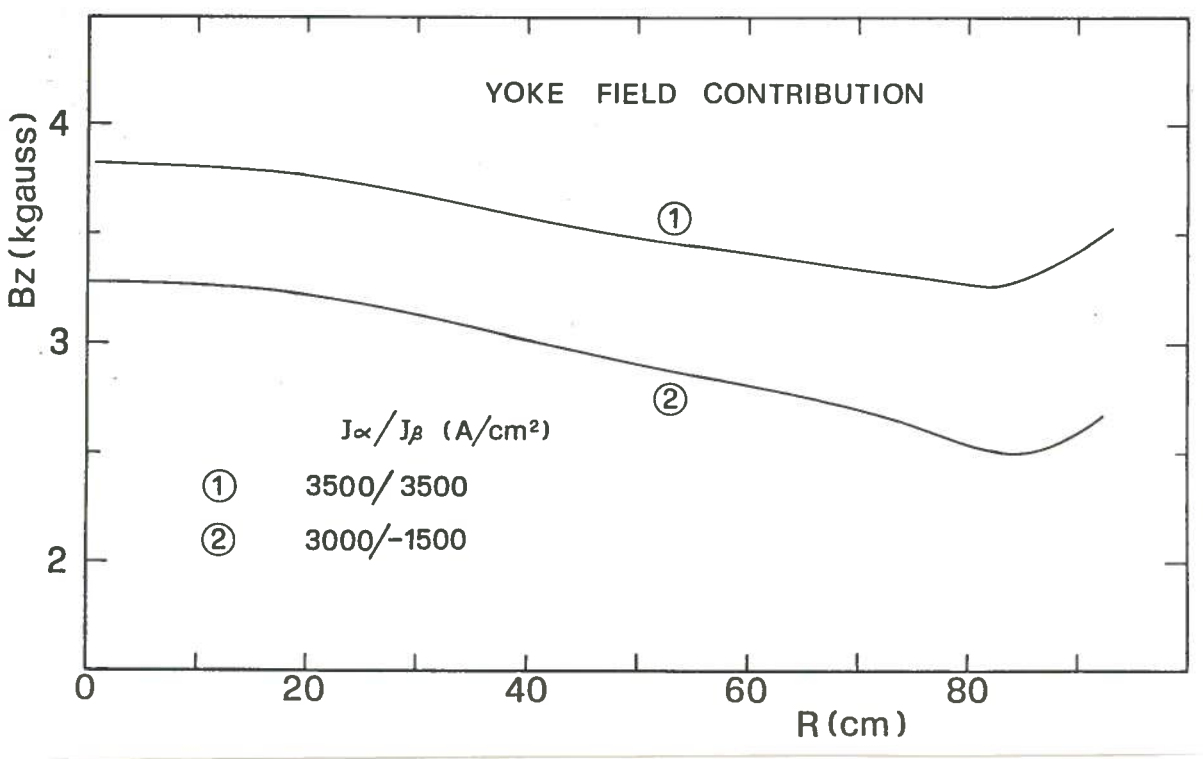

FIG. 5 - Yoke field contribution at the midplane at two different main coils excitations.

The excitation $J_\alpha = J_\beta = 3500$ A/cm^2 corresponds roughly to the maximum cyclotron operating field ($\sim$50 kGauss) while $J_\alpha = 3000$, $J_\beta = -1500$ A/cm^2 corresponds to a field level of about 30 kGauss which has the strongest radial field gradient, as needed for the acceleration of fully stripped light ions to the maximum energy. The yoke field level does not change substantially with the main coil excitation and has a practically constant negative gradient of the order of - 15 Gauss/cm.

We point out that, due to the smooth behaviour of the yoke field contribution, the B_y component outside the midplane in the region occupied by the trim coils should be small compared to the same field component produced by the main coils and by the pole sectors.

An example of the B_r, B_z coil field components at two radii, corresponding to the mid-region and to the extraction region of the cyclotron is presented in Fig. 6 for both main coils excitations as a function of the distance from the midplane. As apparent from the figure there is almost a factor two between the two B_z field levels at the indicated excitations but the field is however essentially constant along the Z direction.

The B_r field component at R = 50 cm is a linear function of the distance from the midplane and practically independent from the coils excitation. At R = 85 cm higher order effects appear and the B_r field is a factor three higher for the lower excitation. This is due to the fact that the latter is obtained with opposed currents in the two main coils sections.

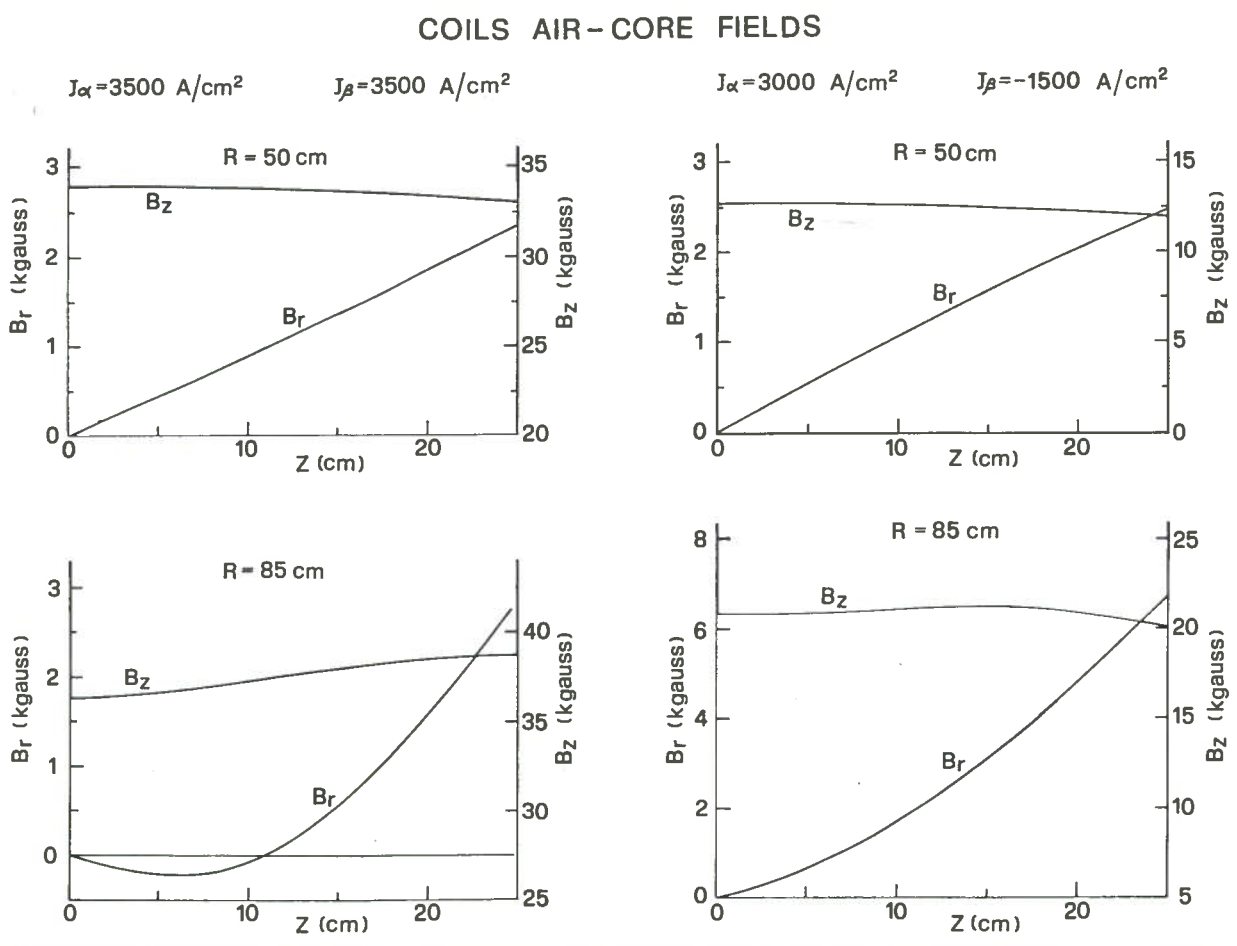

FIG. 6 - B_r, B_z field components produced by the main coils at two different radii and two different excitations as a function of the distance from the median plane.

The magnetic field generated by the poles and the poles sectors (see Fig. 3) in the region occupied by the trim coils is shown in Figs. 7 and 8. All the three field components have been evaluated and the one not relevant for the forces on the trim coils is plotted as a dashed line. The figures present also a schematic cross section of the hill at the specified radii.

We point out that the coordinate system r, ϑ, z employed is a left handed system (see Fig. 2) so that the ϑ coordinate increases following the motion of the accelerated ions in the cyclotron.

The general features of the field are a practically constant B_z field level of about 20 kGauss in the main gap (8.6 cm) between the hill across the midplane and in the small gap (1.5 cm) between the two hill parts and a very small B_z field level of the order of 5 kGauss along the hill sides. Strong B_r, B_ϑ components appear at the edges of the hill reaching values of the order of 5 kGauss at the edges close to the midplane.

Referring to Fig. 7, namely to a radius of 50 cm which corresponds to the mid-region of the cyclotron, a high degree of symmetry for the B_r, B_ϑ field components

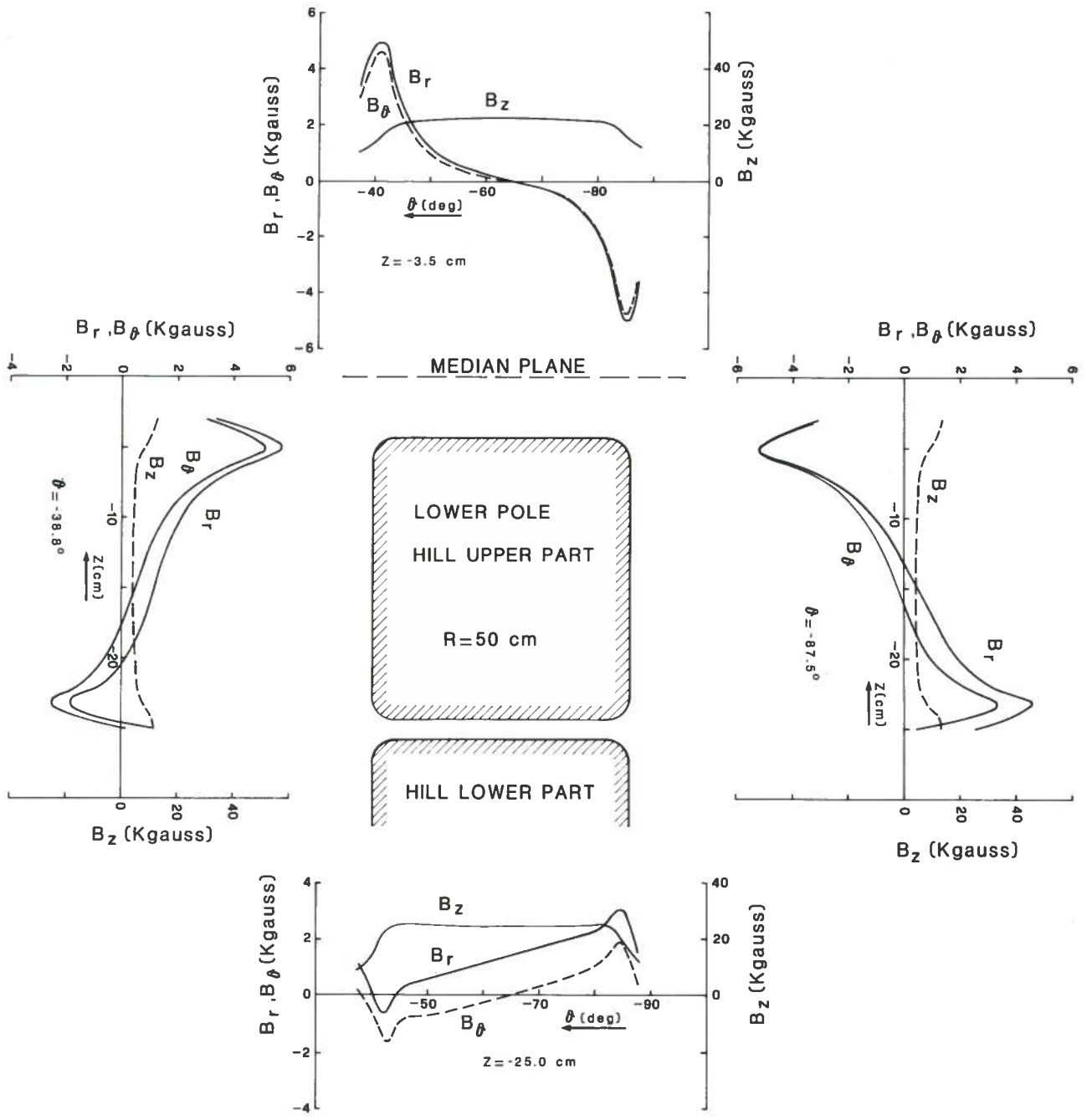

FIG. 7 - B_r, B_ϑ, B_Z field components produced on the T. C. position at R = 50 cm by the saturated pole tips.

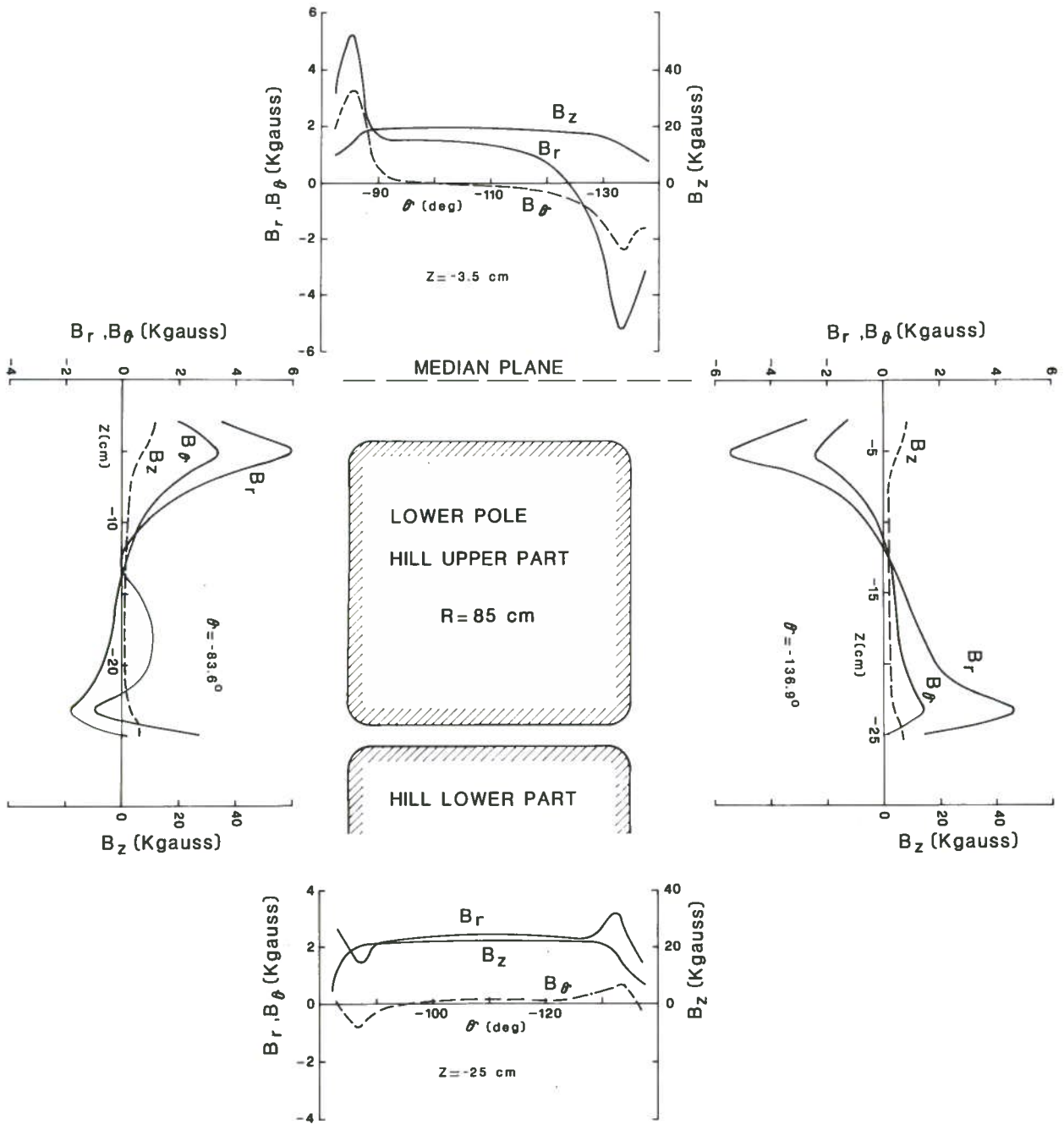

FIG. 8 - B_r, B_ϑ, B_z field components produced on the T.C. position at R = 85 cm by the saturated pole tips.

is present. This can be expected considering that γ, the angle between the circle of 50 cm radius and the hill profile, is about 46^{o} which implies at first order the equality of the B_r and B_ϑ components according to the formula

$$B_r/B_\vartheta = \text{tg}\ \gamma .$$

At the radius R = 85 cm, close to the extraction region, the B_ϑ component is still quite symmetric with respect to the hill center and approximately in the right ratio with the B_r component according to the formula given above with $\gamma = 65^{o}$.

The B_r component instead is quite asymmetric with respect to the hill center line, due to the proximity of the pole edge (pole radius R = 90 cm) where strong flux leakages do obviously exist.

We also note that the B_r field on the left side of the hill presents a strange bulge in the region between z = - 15 and z = - 20 cm. One possible explanation is the proximity to the edge of the valley skirt which extends radially from R = 87. 5 to R = 90 cm and axially up to 12. 5 cm from the midplane (see Fig. 3).

4. - FORCES CALCULATION.

Four loops, each one carrying the nominal current of the trim coil cable, have been selected as representative of the overall behaviour of the trim coil windings. Their radii are 15, 50, 80, 85 cm and are close to the average radii of the trim coils N. 2, 11, 19, 20 whose values are respectively 15. 1, 49. 9, 80. 5, 84. 6 cm.

Each loop is formed by two circular arcs, placed at z = - 3. 5 cm and z = - 25 cm from the midplane, with an azimuthal width equal to the average trim coil extension, and two vertical sides connecting the two arcs.

The magnetic field on the loop has been computed as explained in the previous section and the corresponding forces have been evaluated with the formula (2). Two main coil excitations have been considered corresponding roughly to the minimum ($\sim$ 30 kGauss) and maximum ($\sim$ 50 kGauss) operating field of the cyclotron.

We further recall that the coordinates r, ϑ, z indicated in the figures form a left handed system.

The resulting forces distribution along all the sides of a loop placed at R = 50 cm is presented in Fig. 9 for a current of 400 A, at the maximum main coil excitation.

As it appears from the figure the forces diagram closely resembles the magnetic field distribution produced by the pole sectors (see Fig. 7). At this radius indeed the B_r component produced by the main coils is a factor two lower than the one produced by

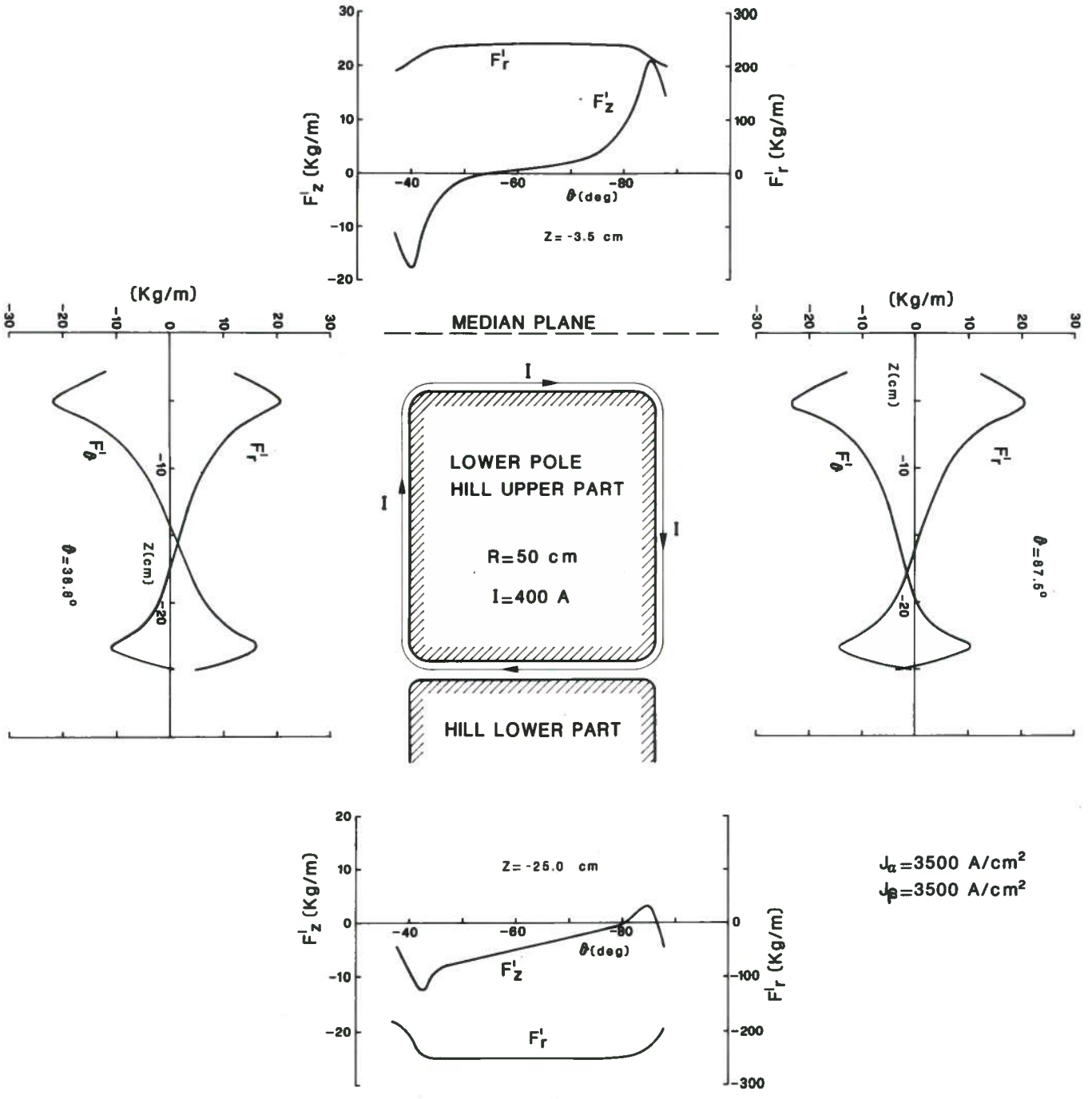

FIG. 9 - Forces distribution on a loop placed at R = 50 cm and carrying 400 A at the indicated main coils excitation.

the sectors. The main coils instead give a substantial contribution (up to 2/3) to the B_z field and this is reflected in the intensity of the radial forces over the hill faces where they reach the value of 250 Kg/m. All the other forces have quite low values and have sharp peaks near the edges of the hill.

The total forces acting on trim coil N. 11 have been computed using the force distribution of the corresponding loop scaled to the maximum number of Ampereturns of the trim coil.

For each side of the trim coil the total force components and their point of application have been calculated in order to visualize the possible torques. For the trim coil N. 11, at the two mentioned main coils excitations, these results are summarized in Fig. 10 where also a cross section of the hill and the equivalent loop used for the calculation is shown.

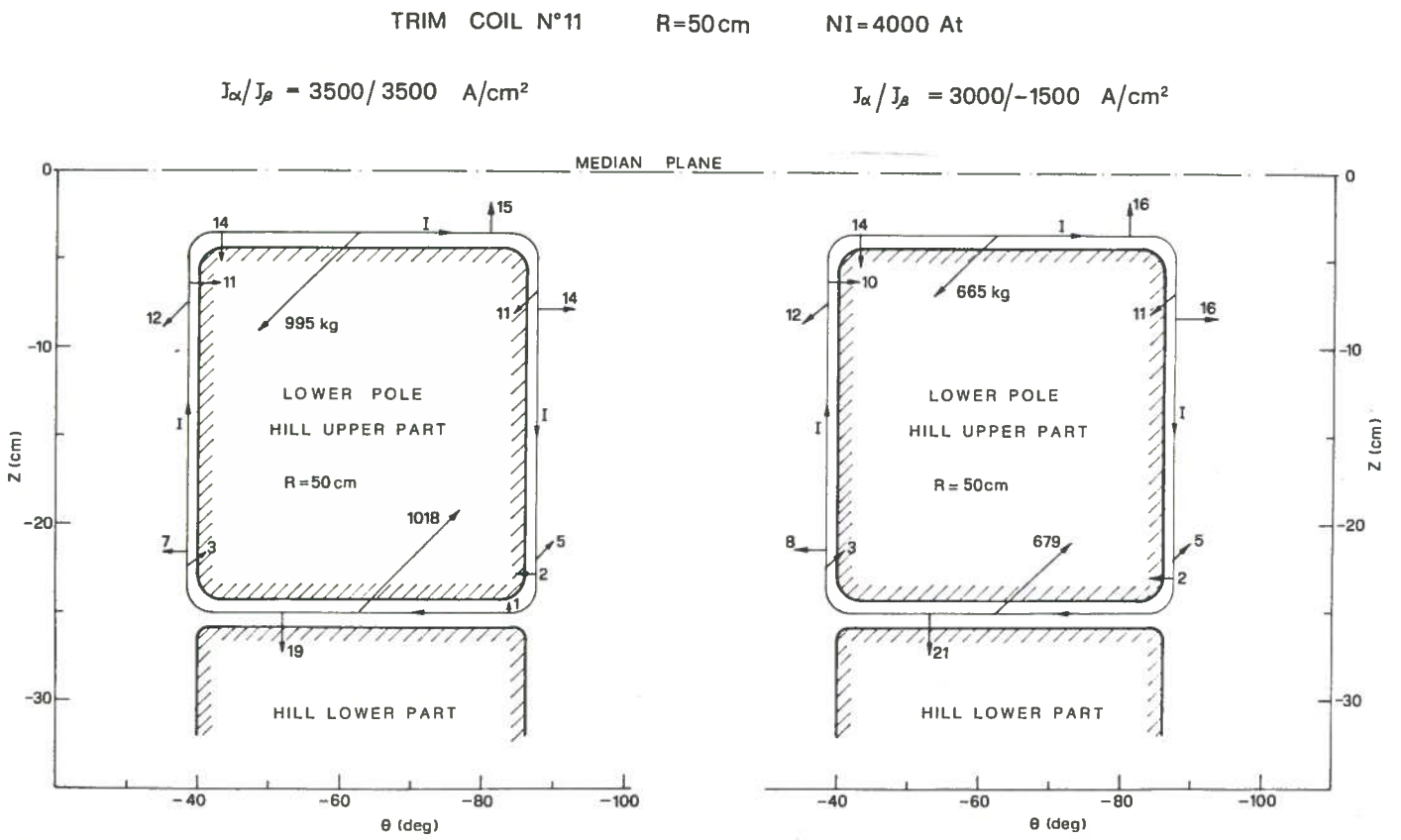

FIG. 10 - Total forces (in Kg) applied on the trim coil N. 11 for two different main coils excitations.

As expected a strong torque around the ϑ axis exists plus other small torques and forces on all the sides of the trim coils.

No substantial difference exists between the two main coil excitations apart from the obvious scaling of the torque with the B_z field. Similar diagrams are presented in Figs. 11, 12, 13 respectively for the trim coil N. 2, 19, 20.

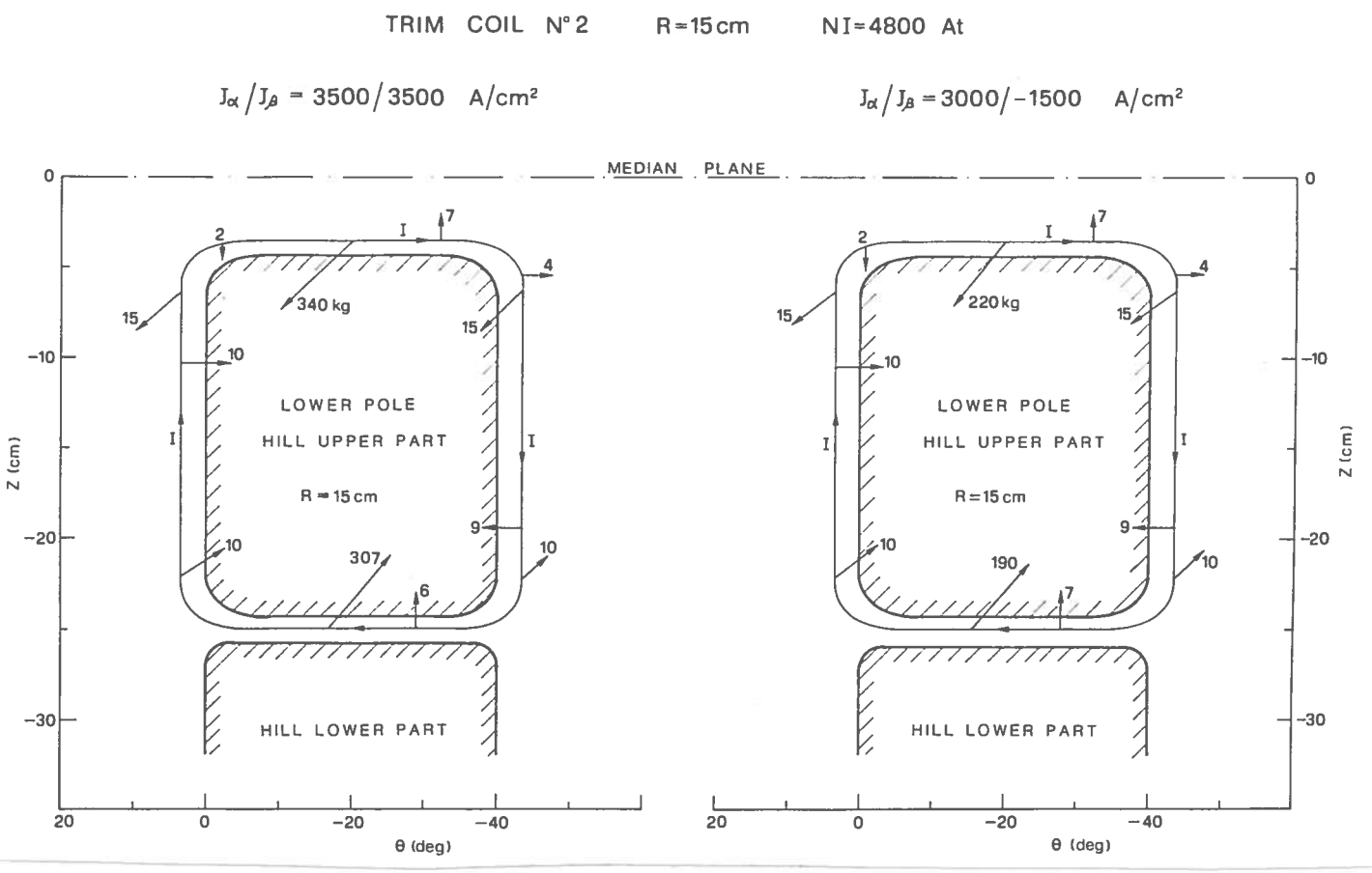

FIG. 11 - Total forces (in Kg) applied on the trim coil N. 2 for two different main coils excitations.

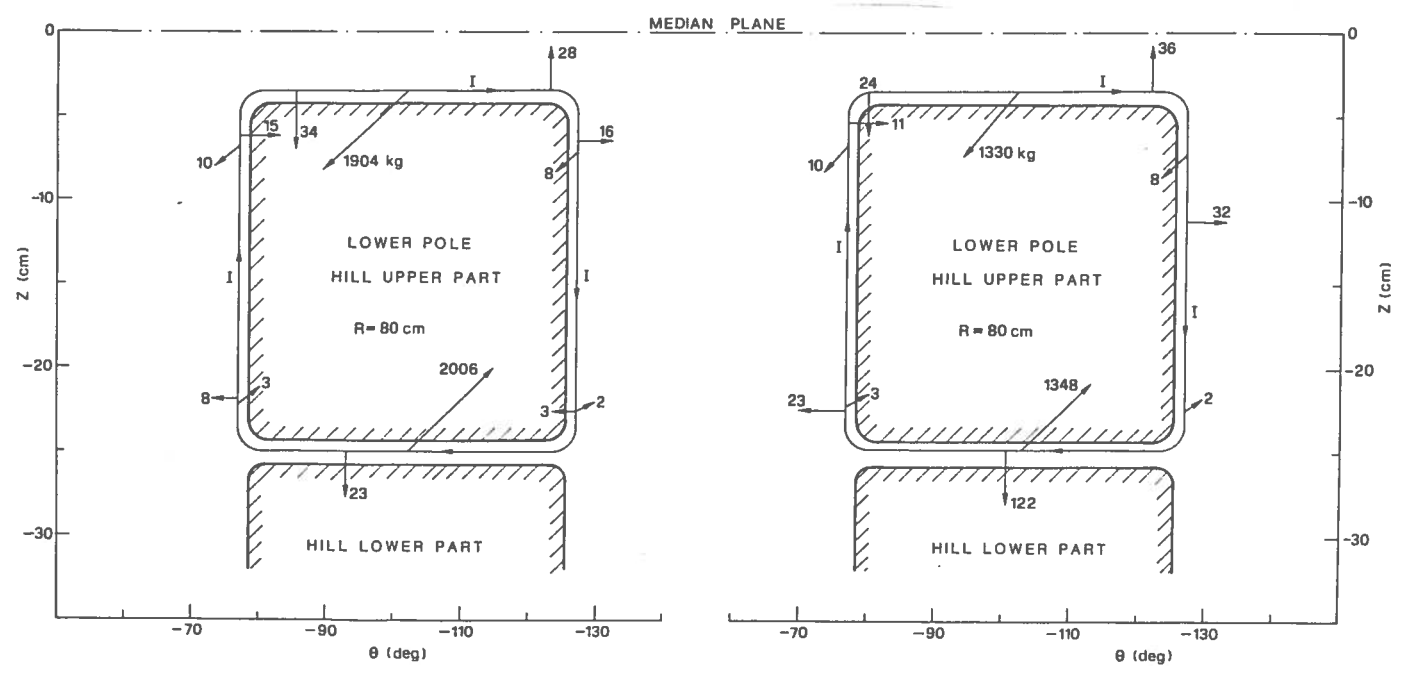

FIG. 12 - Total forces (in Kg) applied on the trim coil N. 19 for two different main coils excitations.

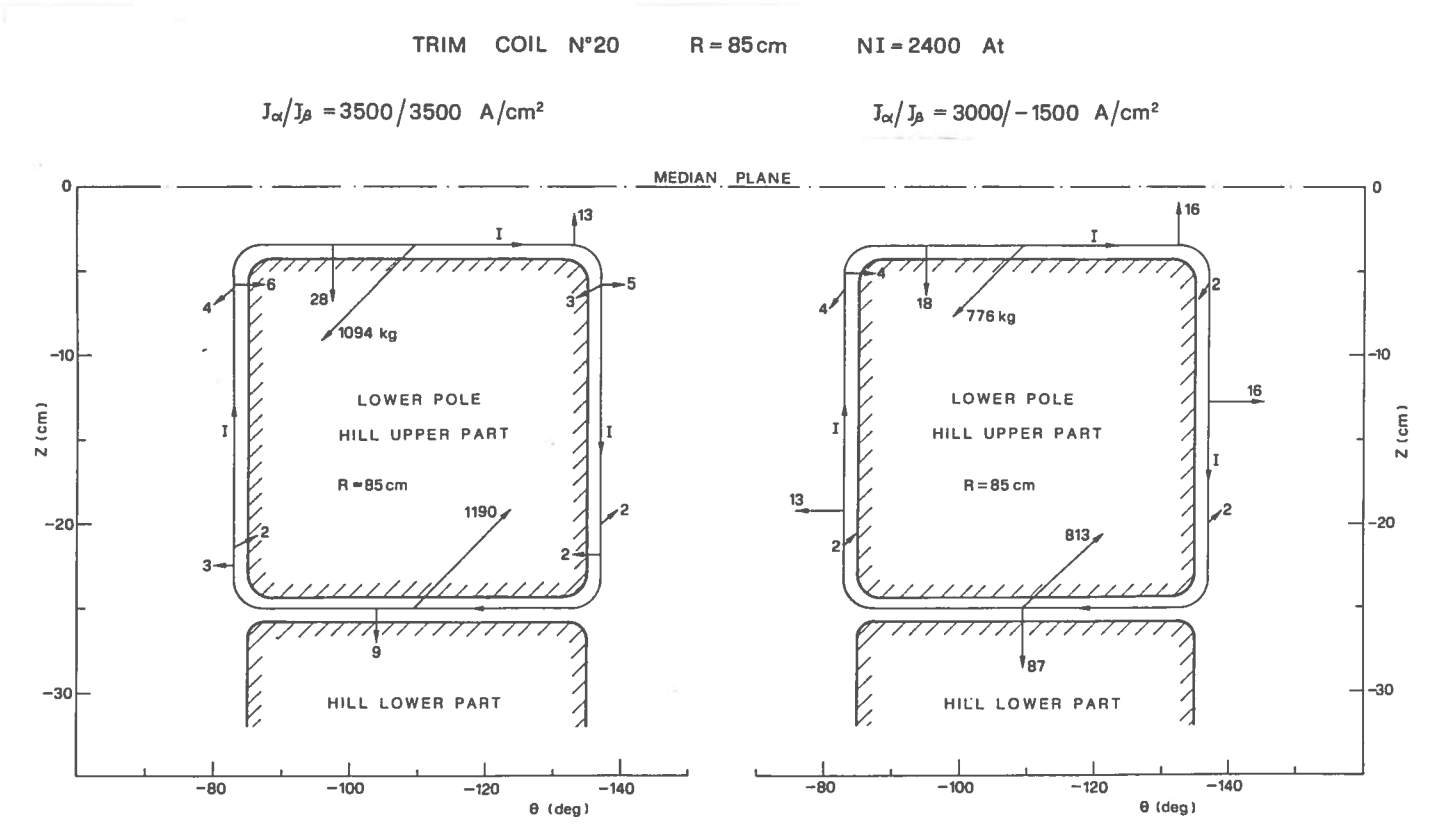

FIG. 13 - Total forces (in Kg) applied to the trim coil N. 20 for two different main coils excitations.

Concerning trim coil N. 2 (Fig. 11) we note that the forces on the vertical side of the coil are quite small because of the small B_r and B_ϑ components produced either by the main coils and pole sectors.

We remark that the trim coil N. 20 has a lower maximum excitation since it is made with one layer only (see section 2).

This trim coil does exhibit noticeable differences between the two main coil excitations due, as pointed out in the previous section, to the strong B_r component produced by the coils.

5. - THE TRIM COILS ASSEMBLY.

The trim coil windings, without any impregnation, would have a too low mechanical rigidity to withstand the radial and vertical forces on the horizontal surfaces.

The envisaged solution to prevent either coil deformations or movements is the epoxy impregnation in a single block of each group of four trim coils in between two successive spacers. The block has to be removable in order to allow a possible shimming of the hill or to change damaged trim coils. This will be done by covering the hill with a very thin layer of teflon (or similar material) which will prevent the epoxy to stick to the hill after the impregnation is completed.

The rigidity of the block is very high and consequently the only remaining concern is the shear stress, induced by the radial forces acting on the trim coils, on the screws which fix the radial spacer to the upper part of the hill (see Fig. 4).

The radial forces acting on the trim coils at the maximum operating field (central field value B_o = 48 kGauss) and at the maximum excitation (i. e. 4000 At) are presented in Fig. 14.

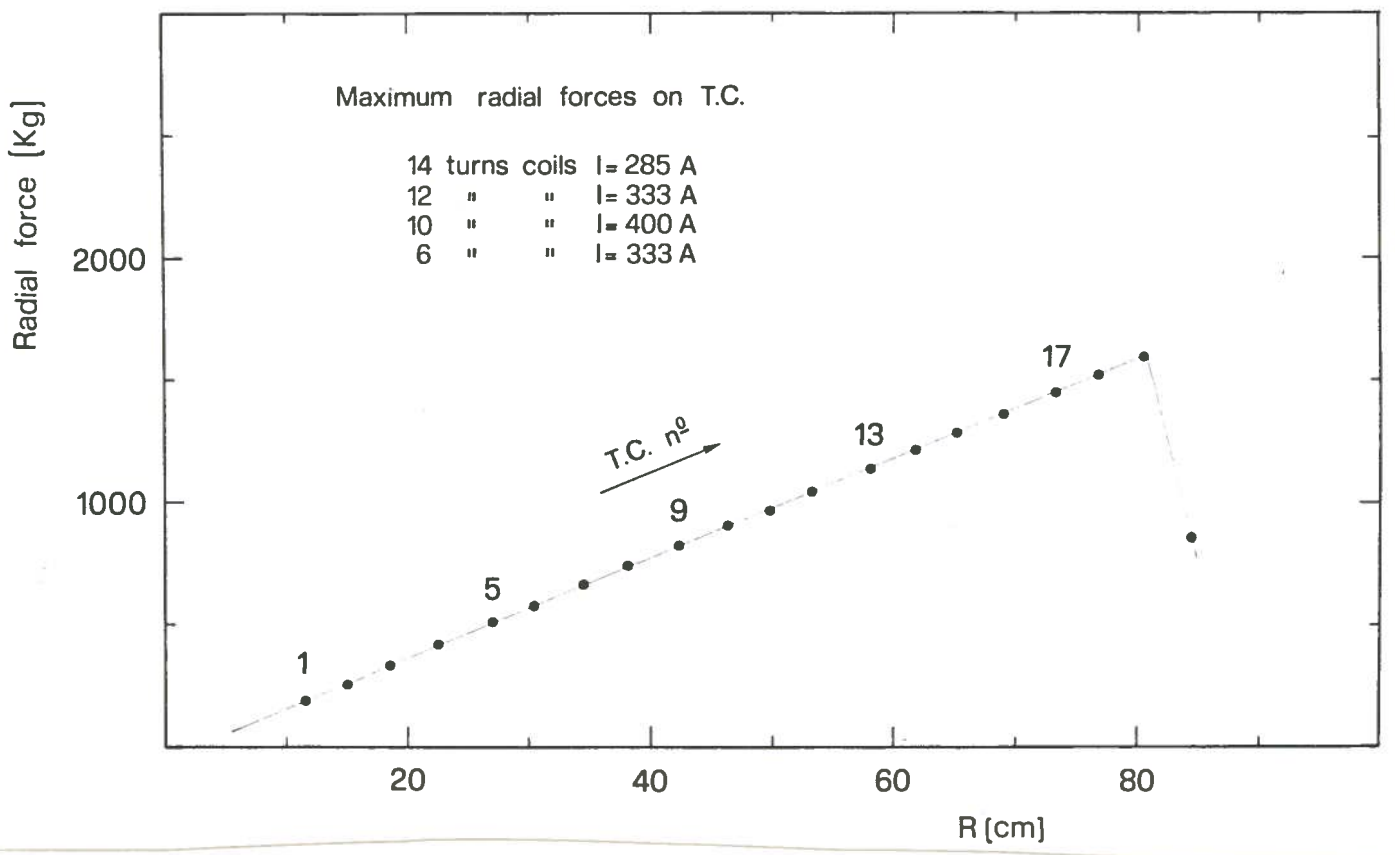

FIG. 14 - Radial forces acting on the T. C. at the maximum operating field (B_o = 48 kGauss) and at the maximum excitation (4000 At).

The linear increase of the force with the T. C. number is substantially due to the equivalent increase of the T. C. azimuthal length with the radius. The full excitation of all the trim coils at the maximum operating fields does not correspond to any real case of trimming operation and therefore the maximum radial forces acting on the T. C. groups cannot be calculated using the data of Fig. 14.

Extensive calculations have been carried out through all the operating diagram of the machine in order to evaluate, for each group of trim coils, the extreme values of the radial forces.

Since the radial forces are proportional to the product BI, where B is the field value at the T. C. location and I the trim coil current, the extremes should correspond to the ions requiring maximum field values and/or trim coil power.

The radial forces for three representative ions satisfying the above criteria (see also Fig. 1) are listed in Table II.

TABLE II - Radial forces (Kg) on the T. C. groups for three ions.

	ION $(Z/A, B_o)$		
T. C. group	0. 05/48	0. 25/45. 5	0. 667/26. 2
1	600	0	- 400
2	2100	300	- 1300
3	3000	400	- 1500
4	1300	- 600	- 2600
5	- 2300	- 2600	2000

Positive values correspond to outward direction respect to the machine center.

The values reported in Table II are relative to the trimming mode operation of the trim coils, and therefore additional forces arise when T. C. (1, 2) or (3, 4) and (19, 20) are used also as harmonic coils.

The maximum absolute values of the radial forces when considering also the maximum trim coil excitation foreseen for the harmonic mode operation are reported in Table III.

TABLE III - Forces on the spacers.

T. C. group and spacer	F_r (Kg)	F_r on spacer (Kg/cm^2)	N of screws per spacer	
			minimum	adopted
1	900	41	3	7
2	2100	53	8	10
3	3000	53	11	14
4	1300	18	5	10
5	3600	66	13	20

Since the spacer azimuthal length increases with the radius it is obviously more convenient to fix each T. C. group to the external spacer. This is accomplished by impregnating together in one rigid block the group of four trim coils and the external stainless steel spacer.

The epoxy resin employed for the impregnation should in such a case withstand the magnetic forces indicated in the third column of Table III. We point out that the spacer

is 15 mm high (the last one only 7 mm), 13 mm wide and with the same azimuthal extension of the non tapered portion of the hill (see section 2).

The spacer will be fixed to the upper part of the hill with screws ∅6 H12 which can safely withstand in excess of 10 Kg/mm^2 of shear stress, i. e. 280 Kg per screw.

The minimum and the adopted number of screws per spacer is listed in Table III. The compensation for the screw holes, in order to minimize the magnetic field perturbation thus introduced, will be obtained by placing a small shim, of height 0. 4 or 0. 6 mm, with the same area as the spacer, between the hill surface and the spacer itself.

6. - CONCLUSIONS.

This study has shown that a solution exists for building trim coils, which will safely withstand the anticipated magnetic forces while, at the same, allowing an easy removal and changing of the trim coils themselves.

Prototypes are now being built according to the guidelines presented here. The preliminary results are satisfactory and once terminated they will be subsequently reported.

Nevertheless it is anticipated that, even from a mechanical point of view, the final solution will differ from the one presented here in minor details only.

REFERENCES.

(1) - E. Acerbi et al., The Milan Superconducting Cyclotron Project, Proceedings of the IX Intern. Conf. on Cyclotrons and their Applications, Caen (France) 1981 (Les Editions de Physique, 1981), pag. 169; E. Acerbi et al., Status of the Superconducting Cyclotron Project in Milan, Report INFN/TC-82/12 (1982).

(2) - M. M. Gordon and D. A. Johnson, Calculation of Fields in a Superconducting Cyclotron assuming Uniform Magnetization of the Pole Tips, Particles Accelerators 10, 217 (1980).

(3) - E. Fabrici and F. G. Resmini, Poisson Calculations for the Milan Superconducting Cyclotron, Report INFN/TC (to be published).

(4) - G. Bellomo et al., Magnetic Field Mapping of the K-500 Cyclotron at MSU, Nuclear Instr. and Meth. 180, 285 (1981).